

Impacts of Slips on Peristaltic Flow and Heat Transfer of Micropolar Fluids in an Asymmetric Channel

Adetunji Adeniyani^{1*}, Gbeminiyi M. Sobamowo², Samsondeen O. Kehinde³

^{1*} Department of Mathematics, University of Lagos, Akoka, Nigeria

² Department of Mechanical Engineering, University of Lagos, Akoka, Nigeria

³ Department of Mathematics, University of Lagos, Akoka, Nigeria

*Corresponding author: aadeniyani@unilag.edu.ng, kencom247@gmail.com

Article Info

Received: 27 December 2021 Revised: 9 March 2022

Accepted: 15 March 2022 Available online: 20 March 2022

Abstract

Peristaltic motion research is gaining popularity in the industrial, biological, medical, physiological, and engineering fields. The influence of slips on the flow of peristaltic and heat transfer of micropolar fluids in an asymmetric channel is studied analytically in this work. The model governing the equations are studied under the long wave and low Reynolds number approximations. Using similarity transformation, the generated nonlinear coupled partial differential equations are turned into nonlinear ordinary differential equations, along side the boundary conditions. Solutions are sought analytically by means of differential transformation method for the cases when the thermal and variable viscosity parameters are present. According to the findings, viscosity and thermal slips improve the flow of the bolus as it travels through the digestive tract. The impact of microrotation also aids in lowering the flow's pressure gradient..

Keywords: Peristaltic; Micropolar; Asymmetric channel; Analytic solutions.

MSC2010: 76P05.

1 Introduction

Peristalsis is a sequence of wave-like muscular contractions that convey fluid-like substances along the digestive tract to separate processing stations. It is derived from the Greek word *peristellein*, which means "to wrap around." It was invented in New Latin. When a bolus of food is ingested, the process of peristalsis begins in the oesophagus. The smooth muscle in the oesophagus makes strong wave-like motions that transport food to the stomach, where it is churned into a liquid combination known as "chyme." Smooth muscle tissue contracts in sequence in much of a digestive tract, such as the human gastrointestinal tract, to produce a peristaltic wave, which propels a ball of food (called a bolus while in the oesophagus and upper gastrointestinal tract and chyme after being churned in the stomach) along the tract [1]. Circular smooth muscle relaxation is followed by contraction behind the chewed material to keep it from travelling backward, and then longitudinal contraction to propel it forward. Peristalsis continues in the small intestine, where it mixes and pushes the

chyme back and forth, allowing nutrients to be absorbed into the bloodstream through the millions of villi and micro-villi that line the walls of the small intestine. Peristalsis comes to a halt in the large intestine, where the water from the undigested meal is absorbed into the bloodstream. Finally, the body's leftover waste materials are expelled through the rectum via anus. Because the human lymphatic system lacks a central pump, peristalsis is responsible for the circulation of lymph and the valves in capillaries. Peristalsis is the natural flow of sperm from the testicles to the urethra. The earthworm is a limbless annelid worm with a peristalsis-driven hydrostatic skeleton. It has a fluid-filled body cavity surrounded by extendable body walls in its hydrostatic skeleton. The worm travels by radially contracting the anterior section of its body, causing hydrostatic pressure to cause an increase in length. The worm's body is restricted in this area, which propagates posterior. As a result, each segment extends forward, relaxes, and re-contacts the substrate, with a hair-like set that prevents retrograde sliding.

A peristaltic pump is a positive-displacement pump that works by pinching advancing parts of a flexible tube to move fluid through it. The pump separates the fluid from the machinery, which is critical if the fluid is abrasive or needs to be kept sterile. Peristalsis has been used by robots to achieve locomotion in the same way that it is used by earthworms. Peristaltic pumps are utilized in a wide range of applications. They're utilized in printing inks and dyes, mining slurring, waste water slurring, bleach, sodium bromide, and lime slurry pumping, among other things. Suction lift applications are also a good fit for peristaltic pumps. They evolve and improve in the same way that all other technologies do. Shoe design restrictions and inadequate rubber technologies hampered early designs.

The necessity to model the flow of fluids containing rotating micro-constituents led to the development of micropolar fluid theory. A micropolar fluid is one with internal structures that takes into account the interaction between the spin of each particle and the macroscopic velocity field. It is a hydrodynamical framework designed for granular systems with macroscopic-sized particles. Eringen [2] was the first to put the theory of micropolar fluids into words. Many researchers [3–12] have worked on micropolar fluids, including applications of microrotation fluid, slip effect, magneto-Micropolar fluid, and many more.

The influence of magnetic fields on peristaltic mechanisms is significant in the context of particular issues involving the flow of conductive physiological fluids, such as blood pumping equipment. The effects of a magnetic field on peristaltic flow have been discussed by a number of researchers [6–8, 10, 12–14], and many more. There are few attempts in which the effects of variable viscosity in the peristaltic mechanisms are considered. Mention may be made of the interesting works of Shit and Roy [8] and Ali et al. [3]. The variable viscosity is considered to be a function of space (height). In a typical situation most of the fluids have temperature dependent viscosity and this property varies significantly when large temperature difference manifests. Khan et al. [15] considered variable viscosity of a Jeffrey fluid through a porous medium in an asymmetric channel while Rao and Mishra [16] discuss the viscous flow in an asymmetric channel. Massoudi and Christie [17] studied the effects of variable viscosity for a simple pipe flow of a third grade fluid. Later Pakdemirli and Yilbas [18] and Pandey and Chaube [14] examined the temperature dependent viscosity. The goal of this study is to see how slip affects Micropolar fluid peristaltic flow and heat transfer in an asymmetric channel with varying viscosity and thermal conductivity. Under the premise of a long wave-length and low Reynolds number, the similarity transformation was employed to convert the governing nonlinear partial differential equations to nonlinear ordinary differential equations. Axial velocity, microrotation component, wall shear stresses, stream function, and pressure gradient were all solved using the Differential Transformation Method. The problem's consequences of various physical characteristics are visually presented.

2 Mathematical Formulation

Consider the flow of a non-uniform porous channel of uniform thickness of length $2a$ through an unstable, incompressible, viscous, and electrically conducting micropolar fluid under the influence of an external magnetic field as seen in Figure 1. Temperature distributions on the upper and lower walls ensure that convective conditions are met. Let $Y = h(X, t)$ denote the distance between the upper and lower walls of the channel, which is thought to be produced by a sinusoidal wave train propagating along the length of the channel wall at a wave speed of c , such that

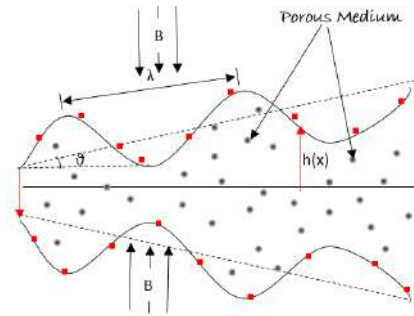


Figure 1: A physical representation of the model

||

$$h(X, t) = a + (X - ct) \tan \vartheta + b \sin \left(\frac{2\pi}{\lambda} (X - ct) \right) \quad (2.1)$$

where a is the channel's half width at the entrance, λ is the wave length, b is the amplitude of the wave, ϑ is the angle between the channel's axis and the walls, and X and Y are rectangular co-ordinates, with X being the channel's axis and Y being the traverse axis perpendicular to X whereas t signifies the time. Because the system is strained by an external transverse magnetic field of intensity, the total magnetic field induction vector is $\mathbf{B}(0, B_0, 0)$, with the induced magnetic field ignored due to the assumption of low electrical conductivity. By ignoring the body couplings, the equations of motion for unsteady flow through porous medium of an incompressible magneto-micropolar fluid with externally imposed magnetic field are as seen in [6]:

$$\nabla \cdot \mathbf{V} = 0 \quad (2.2)$$

$$\rho \left(\frac{\partial \mathbf{V}}{\partial t} + \mathbf{V} \cdot \nabla \mathbf{V} \right) = -\nabla \bar{p} + (\mu + \kappa) \nabla^2 \mathbf{V} + \kappa (\nabla \wedge \boldsymbol{\Omega}) + \mathbf{J} \wedge \mathbf{B} - \frac{(\mu + \kappa)}{K_p} \mathbf{V} \quad (2.3)$$

$$\rho \bar{j} \left(\frac{\partial \boldsymbol{\Omega}}{\partial t} + \mathbf{V} \cdot \nabla \boldsymbol{\Omega} \right) = -2\kappa \boldsymbol{\Omega} + \kappa \nabla \wedge \mathbf{V} + (\mu + \kappa) \nabla^2 \mathbf{V} \wedge \mathbf{V} - \gamma (\nabla \wedge \nabla \wedge \boldsymbol{\Omega}) + (\alpha + \beta + \gamma) \nabla (\nabla \cdot \boldsymbol{\Omega}) \quad (2.4)$$

and the energy equation is

$$\rho C_p \left(\frac{\partial \bar{T}}{\partial t} + \mathbf{V} \cdot \nabla \bar{T} \right) = \kappa \nabla^2 \bar{T} + Q_0 (\bar{T} - T_0) \quad (2.5)$$

as well as the generalized ohm's law $\mathbf{J} = \sigma(\mathbf{E} + \mathbf{V} \wedge \mathbf{B})$. where $\mathbf{V} = (\bar{u}, \bar{v}, 0)$ is the velocity vector, $\boldsymbol{\Omega} = (0, 0, \bar{N}(\bar{x}, \bar{y}))$ the microrotation vector, \bar{p} is the total fluid pressure, μ is the kinematic viscosity

of the fluid, $\frac{\partial}{\partial \bar{t}}$ is the local material time derivative, \bar{t} is the time, $\bar{\rho}$ the fluid density, \bar{j} the micro gyration parameter, \mathbf{J} current density vector, σ electrical conductivity of the fluid and \mathbf{E} is the electric field vector. Also, κ , α , β and γ are the material constants (viscosity coefficients of the micropolar fluid)

The following relationships can be used to translate the current phenomenon from the laboratory to the wave frame.

$$\bar{x} = \bar{X} - c\bar{t}, \bar{y} = \bar{Y}, \bar{u} = \bar{U} - c, \bar{v} = \bar{V}, \bar{w} = \bar{N}, \bar{p}(\bar{x}, \bar{y}) = p(\bar{X}, \bar{Y}, \bar{t})$$

where c is the wave's propagation speed.

We have the following formulas using the provided values of the velocity field:

$$\frac{\partial \bar{u}}{\partial \bar{x}} + \frac{\partial \bar{v}}{\partial \bar{y}} = 0 \quad (2.6)$$

$$\begin{aligned} \rho \left(\frac{\partial}{\partial \bar{t}} + (\bar{u} + c) \frac{\partial}{\partial \bar{x}} + \bar{v} \frac{\partial}{\partial \bar{y}} \right) (\bar{u} + c) &= -\frac{\partial \bar{p}}{\partial \bar{x}} + (\bar{\mu} + \kappa) \left(\frac{\partial^2}{\partial \bar{x}^2} + \frac{\partial^2}{\partial \bar{y}^2} \right) (\bar{u} + c) \\ &+ \left(\frac{\partial \bar{\mu}}{\partial \bar{x}} \frac{\partial}{\partial \bar{x}} + \frac{\partial \bar{\mu}}{\partial \bar{y}} \frac{\partial}{\partial \bar{y}} \right) (\bar{u} + c) + \kappa \frac{\partial \bar{w}}{\partial \bar{y}} - \sigma B_0^2 (\bar{u} + c) - \frac{(\bar{\mu} + \kappa)}{k_p} (\bar{u} + c) \end{aligned} \quad (2.7)$$

$$\begin{aligned} \rho \left(\frac{\partial}{\partial \bar{t}} + (\bar{u} + c) \frac{\partial}{\partial \bar{x}} + \bar{v} \frac{\partial}{\partial \bar{y}} \right) \bar{v} &= -\frac{\partial \bar{p}}{\partial \bar{y}} + (\bar{\mu} + \kappa) \left(\frac{\partial^2}{\partial \bar{x}^2} + \frac{\partial^2}{\partial \bar{y}^2} \right) \bar{v} \\ &+ \left(\frac{\partial \bar{\mu}}{\partial \bar{x}} \frac{\partial}{\partial \bar{x}} + \frac{\partial \bar{\mu}}{\partial \bar{y}} \frac{\partial}{\partial \bar{y}} \right) \bar{v} - \kappa \frac{\partial \bar{w}}{\partial \bar{x}} - \frac{(\bar{\mu} + \kappa)}{K_p} \bar{v} \end{aligned} \quad (2.8)$$

$$\rho \bar{j} \left(\frac{\partial}{\partial \bar{t}} + (\bar{u} + c) \frac{\partial}{\partial \bar{x}} + \bar{v} \frac{\partial}{\partial \bar{y}} \right) \bar{w} = \gamma \frac{\partial^2 \bar{w}}{\partial \bar{y}^2} - \kappa \left(2\bar{w} + \frac{\partial \bar{u}}{\partial \bar{y}} \right) \quad (2.9)$$

The energy equation is

$$\rho C_p \left(\frac{\partial}{\partial \bar{t}} + (\bar{u} + c) \frac{\partial}{\partial \bar{x}} + \bar{v} \frac{\partial}{\partial \bar{y}} \right) \bar{T} = \frac{\partial}{\partial \bar{x}} \left(\bar{k} \frac{\partial \bar{T}}{\partial \bar{x}} \right) + \frac{\partial}{\partial \bar{y}} \left(\bar{k} \frac{\partial \bar{T}}{\partial \bar{y}} \right) + Q_0 (\bar{T} - T_0) \quad (2.10)$$

where C_p the specific heat, \bar{T} temperature, $\mu(\bar{T})$ changeable viscosity, k variable thermal conductivity, Q_0 constant heat addition/absorption, and T_0 temperature at the lower and upper walls are all taken into account.

Introducing the following dimensionless variables as stated by Shit and Roy [6],

$$\begin{aligned} x = \frac{\bar{x}}{\lambda}, y = \frac{\bar{y}}{a}, u = \frac{\bar{u}}{c}, v = \frac{\bar{v}}{c\delta}, t = \frac{c\bar{t}}{\lambda}, j = \frac{\bar{j}}{a^2}, \delta = \frac{a}{\lambda}, p = \frac{a^2 \bar{p}}{\mu_0 c \lambda}, h = \frac{\bar{h}}{a}, \phi = \frac{b}{a} \\ w = \frac{a \bar{w}}{c}, k_p = \frac{\bar{k}_p}{a^2}, k = \frac{\bar{k}}{\mu_0}, \mu(\theta) = \frac{\mu(\bar{T})}{\mu_0}, k(\theta) = \frac{k(\bar{T})}{k_0}, \theta = \frac{\bar{T} - T_0}{T_1 - T_0} \end{aligned} \quad (2.11)$$

Substituting equation (2.11) into equations (2.6) – (2.10) to obtain

$$\frac{\partial u}{\partial x} + \frac{\partial v}{\partial y} = 0 \quad (2.12)$$

$$\begin{aligned} Re\delta \left(\frac{\partial}{\partial t} + (u+1) \frac{\partial}{\partial x} + v \frac{\partial}{\partial y} \right) (u+1) &= -\frac{\partial p}{\partial x} + (\mu(\theta) + k) \left(\delta^2 \frac{\partial^2 u}{\partial x^2} + \frac{\partial^2 u}{\partial y^2} \right) + \\ &\left(\delta^2 \frac{\partial \mu(\theta)}{\partial x} \frac{\partial u}{\partial x} + \frac{\partial \mu(\theta)}{\partial y} \frac{\partial u}{\partial y} \right) + k \frac{\partial w}{\partial y} - Ha^2 (u+1) - \frac{(\mu(\theta) + k)}{k_p} (u+1) + G_r \theta \end{aligned} \quad (2.13)$$

$$\begin{aligned}
 Re\delta^3 \left(\frac{\partial}{\partial t} + (u+1) \frac{\partial}{\partial x} + v \frac{\partial}{\partial y} \right) v &= -\frac{\partial p}{\partial y} + \delta^2 (\mu(\theta) + k) \left(\delta^2 \frac{\partial^2 v}{\partial x^2} + \frac{\partial^2 v}{\partial y^2} \right) \\
 &+ \delta^2 \left(\delta^2 \frac{\partial \mu(\theta)}{\partial x} \frac{\partial v}{\partial x} + \frac{\partial \mu(\theta)}{\partial y} \frac{\partial v}{\partial y} \right) - \delta^2 \frac{\partial w}{\partial x} - \delta^2 \frac{(\mu(\theta) + k)}{k_p} v
 \end{aligned} \tag{2.14}$$

$$Re\delta \left(\frac{\partial}{\partial t} + (u+1) \frac{\partial}{\partial x} + v \frac{\partial}{\partial y} \right) \theta = \frac{\delta^2}{P_r} \frac{\partial}{\partial x} \left(k(\theta) \frac{\partial \theta}{\partial x} \right) + \frac{1}{P_r} \frac{\partial}{\partial y} \left(k(\theta) \frac{\partial \theta}{\partial y} \right) + \beta_r \theta^r \tag{2.15}$$

$$Re\delta \left(\frac{\partial}{\partial t} + (u+1) \frac{\partial}{\partial x} + v \frac{\partial}{\partial y} \right) w = M \frac{\partial^2 w}{\partial y^2} - K \left(2w + \frac{\partial u}{\partial y} \right) \tag{2.16}$$

Where

$$\begin{aligned}
 Re &= \frac{\rho c a}{\mu_0}, H_a^2 = \frac{\sigma a^2 B_0^2}{\mu_0}, \beta_r = \frac{Q_0 a^2}{\mu_0 C_p (T_1 - T_0)^{1-r}}, G_r = \frac{\rho \alpha g a^2 (T_1 - T_0)}{\mu_0 c}, \\
 p_r &= \frac{\mu_0 c_p}{k_0}, M = \frac{\gamma}{\mu_0 a^2}
 \end{aligned} \tag{2.17}$$

Re is Reynold's number, H_a magnetic parameter (Hartman number), G_r Grashof number, P_r Prandtl number, M micropolar parameter, and β_r heat generation/absorption rate of order r .

In the wave frame, the non-dimensional boundary conditions for the dimensionless velocity u , microrotation component, and stream function $\psi(x, y)$ are as follows:

$$\begin{aligned}
 u \pm \zeta \frac{\partial u}{\partial y} &= -1 \text{ at } y = \pm h(x), \\
 w &= 0 \text{ at } y = \pm h(x), \psi = 0 \text{ at } y = 0 \\
 \text{and } \theta'(0) &= 0, \theta(h) = 1
 \end{aligned} \tag{2.18}$$

Assuming a long wavelength and low Reynolds number in equations (2.13) – (2.17) above and neglecting high powers of δ , we obtain;

$$\frac{\partial p}{\partial x} = (\mu(\theta) + K) \frac{\partial^2 u}{\partial y^2} + \frac{\partial \mu(\theta)}{\partial y} \frac{\partial u}{\partial y} + K \frac{\partial w}{\partial y} - \left(Ha^2 + \frac{\mu(\theta) + K}{k_p} \right) (u+1) + G_r \theta \tag{2.19}$$

$$\frac{\partial p}{\partial y} = 0 \tag{2.20}$$

$$\frac{1}{P_r} \frac{\partial}{\partial y} \left(k(\theta) \frac{\partial \theta}{\partial y} \right) + \beta_r \theta^r = 0 \tag{2.21}$$

$$M \frac{\partial^2 w}{\partial y^2} - K \left(2w + \frac{\partial u}{\partial y} \right) = 0 \tag{2.22}$$

equation (2.20) shows that the pressure only depends on x .

Introducing the Reynold's models along with linear variation of viscosity parameter and thermal conductivity parameter as stated by Balachandra, et.al. (2021) [19] and Fatunmbi, et.al. (2021) [20]

$$\mu(\theta) = 1 - \varepsilon_1 \theta \text{ and } k(\theta) = 1 + \varepsilon_2 \theta \tag{2.23}$$

Substituting for $\mu(\theta)$ and $k(\theta)$ in (2.19) and (2.21) to get;

$$\frac{\partial p}{\partial x} = \frac{\partial}{\partial y} \left((1 - \varepsilon_1 \theta) \frac{\partial u}{\partial y} \right) + K \frac{\partial^2 u}{\partial y^2} + K \frac{\partial w}{\partial y} - \left(Ha^2 + \frac{(1 - \varepsilon_1 \theta) + K}{k_p} \right) (u+1) + G_r \theta \tag{2.24}$$

$$\frac{\partial}{\partial y} \left((1 + \varepsilon_2 \theta) \frac{\partial \theta}{\partial y} \right) + \beta_r P_r \theta^r = 0 \tag{2.25}$$

If variable and thermal viscosity parameters are absent (i.e $\varepsilon_1 = \varepsilon_2 = 0$) and Graphof number $G_r = 0$, we arrived at the equations of Shit and Roy [6].

Since the aim of this work is to study the effect of variable and thermal viscosities, $(\varepsilon_1, \varepsilon_2) \neq 0$. Hence, equations (2.22), (2.24) together with equation (2.25) with the associated boundary conditions equation (2.18) will be analysed using DTM.

It is noteworthy to state that the stress tensor in micropolar fluid is not symmetric. Therefore, the dimensionless form of the shear pressure involved within the present problem is given as Shit and Roy (2015) [6] below

$$\tau_{xy} = \frac{du}{dy} - K\omega \quad (2.26)$$

and

$$\tau_{yx} = (1 + K) \frac{du}{dy} + K\omega \quad (2.27)$$

The dimensionless volumetric rate of flow in the wave frame is given as;

$$q = \int_{-h}^h u(y)dy \quad (2.28)$$

In order to obtain the pumping characteristics by means of pressure rise per wavelength, the axial pressure gradient is determined from the Eq.(2.28) as

$$\frac{\partial p}{\partial y} = \frac{q + 2h}{h} \quad (2.29)$$

The non-dimensional expression of pressure rise ΔP is given by,

$$\Delta P = \int_0^1 \frac{\partial p}{\partial x} dx \quad (2.30)$$

3 Differential Transform Method (DTM)

The DTM was first introduced by Zhou in 1986 [21] in solving several issues in electric circuits, and the results supplied exact values of the nth derivative of an analytic function at a place in terms of both known and unknown boundary conditions in a quick way. In their 60-page publication "On the Efficiency of Differential Transformation Method to the Solutions of Large Amplitude Nonlinear Oscillation Systems," Sobamowo, et.al. [22] and Sobamowo et.al. [23]," Sobamowo, et.al. [22] and Sobamowo et.al. cites. This technique creates a polynomial-based analytical answer.

Definition 3.1. A Taylor polynomial of degree n is defined as follows:

$$P_n(x) = \sum_{k=0}^n \frac{1}{k!} (f^k(c))(x - c)^k \quad (3.1)$$

Theorem 3.2. Suppose that the function f has $(n + 1)$ derivatives on the interval for some $r > 0$, and the for all $x \in (c - m, c + m)$ where $R_n(x)$ is the error between $P_n(x)$ and the approximated function $f(x)$. Then, the Taylor series expansion about $x = c$ converges to $f(x)$.

That is:

$$P_n(x) = \sum_{k=0}^{\infty} \frac{1}{k!} (f^k(c))(x - c)^k, \quad \forall x \in (c - m, c + m) \quad (3.2)$$

Suppose that the function $f(x)$ for the $k - th$ derivative is defined as follows;

Table 1: Basic Operation of Differential Transform Method (DTM)

$f(x)$	$F(k)$
$g(x) \pm h(x)$	$G(k) \pm H(k)$
$\alpha g(x)$	$\alpha G(k)$, α is a constant
$\frac{d}{dx}g(x)$	$(k+1)F(k+1)$
$\frac{d^n}{dx^n}g(x)$	$\frac{k!}{(k+n)!}F(k+n)$
$g(x)h(x)$	$\sum_{i=0}^k G(i)H(k-i)$
x^a	$\delta(k-a)$, where $\delta(k-a) = \begin{cases} 1 & k=a \\ 0 & k \neq 0 \end{cases}$
$\exp(ax)$	$\frac{a^k}{k!}$
$(1+x)^a$	$\frac{a(a-1)\cdots(a-k+1)}{k!}$
$\sin(\alpha x + \beta)$	$\frac{\alpha^k}{k!} \sin\left(\frac{\pi k}{k!} + \beta\right)$
$\cos(\alpha x + \beta)$	$\frac{\alpha^k}{k!} \cos\left(\frac{\pi k}{k!} + \beta\right)$
$\sinh(ax)$	$\frac{1}{2k!} (a^k - (-a)^k)$
$\cosh(ax)$	$\frac{1}{2k!} (a^k + (-a)^k)$

$$F(k) = \frac{1}{k!} \left(\frac{d^k f(x)}{dx^k} \right)_{x=x_0} \quad (3.3)$$

or

$$F(k) = \frac{1}{k!} (f^k(x))_{x=x_0} \quad (3.4)$$

Where $f(x)$ is the original function and $F(k)$ is the transformed function.

Definition 3.3. The inverse differential transform $F(k)$ is defined as;

$$f(x) = \sum_{k=0}^{\infty} (x-x_0)^k F(k) \quad (3.5)$$

Substituting equation (3.3) into equation (3.5) to obtain

$$f(x) = \sum_{k=0}^{\infty} (x-x_0)^k \frac{1}{k!} \left(\frac{d^k f(x)}{dx^k} \right)_{x=x_0} \quad (3.6)$$

equation (3.6) is the Taylor series of $f(x)$ at $x = x_0$.

3.1 Applications of DTM

In an attempt to solve the boundary value problems of equations (2.22), (2.24), and (2.25) with the boundary conditions at equation (2.18), we transform the coupled ODEs to DTM as

$$\begin{aligned}
 & (1 + K)(k + 1)(k + 2)U(k + 2) - \varepsilon_1 \sum_{l=0}^k T(l)(k - l + 1)(k - l + 2)U(k - l + 2) - \\
 & \varepsilon_1 \sum_{l=0}^k (l + 1)T(l + 1)(k - l + 1)U(k - l + 1) + K(k + 1)W(k + 1) - \tag{3.7} \\
 & \xi(U(k) + \delta(k)) - \varepsilon_1 \sum_{l=0}^k T(l)U(k - l) + (G_r - \varepsilon_1)T(k) - \frac{\partial p}{\partial x} \delta(k) = 0
 \end{aligned}$$

$$\begin{aligned}
 & (k + 1)(k + 2)T(k + 2) + \varepsilon_2 \sum_{l=0}^k T(l)(k - l + 1)(k - l + 2)T(k - l + 2) \\
 & + \varepsilon_2 \sum_{l=0}^k (l + 1)T(l + 1)(k - l + 1)T(k - l + 1) + \beta_r P_r F(k) = 0 \tag{3.8}
 \end{aligned}$$

and

$$M(k + 1)(k + 2)W(k + 2) - K((k + 1)U(k + 1) + 2W(k)) = 0 \tag{3.9}$$

where $U(k)$, $T(k)$, and $W(k)$ are the transform functions of $u(y)$, $\theta(y)$ and $w(y)$ respectively. $F(k)$ is the transform of θ^r for $r = 0, 1, 2$ and $\xi = Ha^2 - \frac{1+K}{k_p}$. It will be noticed that when the order of the rate of heat absorption/generation is zero or one, i.e ($r = 0, 1$) then, the transform $F(k)$ will be $\delta(k)$ and $T(k)$ respectively. To transform θ^r when $r \neq 0$ or 1, we let perform the following;

Let

$$\begin{aligned}
 f(y) &= \theta^r \\
 \frac{df}{dy} &= r\theta^{r-1}\theta' \\
 \frac{d^2 f}{dy^2} &= (r(r-1)\theta^{r-2}(\theta')^2 + r\theta^{r-1}\theta'') \\
 \theta^2 \frac{d^2 f}{dy^2} &= r(r-1)\theta^r \theta'^2 + r\theta^r \theta \theta'' \\
 \theta^2 \frac{d^2 f}{dy^2} &= r(r-1) f \theta'^2 + r f \theta \theta''
 \end{aligned} \tag{3.10}$$

The boundary conditions satisfying the equation above is

$$f'(0) = 0, f(h) = 1 \tag{3.11}$$

Transforming equation (3.10) when $r = 2$ to DTM to get

$$\begin{aligned}
 (k + 1)(k + 2)F(k + 2) &= 2 \sum_{l=0}^k (l + 1)T(l + 1)(k - l + 1)T(k - l + 1) + \\
 2 \sum_{m=0}^k \sum_{l=0}^m T(l)(m - l + 1)T(m - l + 1)(k - m + 1)(k - m + 2)T(k - m + 2) \tag{3.12}
 \end{aligned}$$

The boundary conditions for transformed equations (3.7), (3.8), (3.9) and (3.12) are;

$$\begin{aligned}
 U(0) &= a, U(1) = b, W(0) = c, W(1) = d, T(0) = e, T(1) = 0, F(0) = g \\
 F(1) &= 0 \tag{3.13}
 \end{aligned}$$

where a, b, c, d, e , and g are constants which will be evaluated by substituting the boundary conditions in (2.18) into the series solutions gotten from the transform DTM. The term by term of (3.7), (3.8), (3.9) and the boundary condition (3.12) are given below;

$$\begin{aligned}
 U(0) &= a, U(1) = b, U(2) = \frac{-c(a\epsilon_1 + G_r) - Ke + (a+1)\xi + A}{-2\epsilon_1 c + 2K + 2} \\
 U(3) &= -\frac{(c\epsilon_2 + 1)(Mb(\epsilon_1 c - \xi) + K^2(b + 2d)) + MP_r b\beta_r g\epsilon_1}{6M(c\epsilon_2 + 1)(-\epsilon_1 c + K + 1)} \\
 &\quad \left(\begin{aligned}
 &-2MP_r a\beta_r c g\epsilon_1^2 - Mac^3\epsilon_1^2\epsilon_2 - 2G_r MP_r \beta_r c g\epsilon_1 - G_r Mc^3\epsilon_1\epsilon_2 \\
 &-K^2ac^2\epsilon_1\epsilon_2 - 2K^2c^2e\epsilon_1\epsilon_2 - KMP_r a\beta_r g\epsilon_1 - 3KMP_r \beta_r e g\epsilon_1 \\
 &-KMc^2e\epsilon_1\epsilon_2 + 3MP_r a\beta_r g\xi\epsilon_1 + 2Mac^2\xi\epsilon_1\epsilon_2 + 3AMP_r \beta_r g\epsilon_1 \\
 &+ AMc^2\epsilon_1\epsilon_2 - G_r K^2c^2\epsilon_2 - G_r KMP_r \beta_r g + G_r Mc^2\xi\epsilon_2 + K^3ce\epsilon_2 \\
 &+ K^2ac\xi\epsilon_2 + KMc\xi\epsilon_2 - MP_r a\beta_r g\epsilon_1 + 3MP_r \beta_r g\xi\epsilon_1 - Mac^2\epsilon_1^2 \\
 &- Mac\xi^2\epsilon_2 + Mc^2\xi\epsilon_1\epsilon_2 + AK^2c\epsilon_2 - AMc\xi\epsilon_2 - G_r \beta_r P_r gM \\
 &- G_r Mc^2\epsilon_1 - K^2ac\epsilon_1 - 2K^2ce\epsilon_1 + 2K^2ce\epsilon_2 + K^2c\xi\epsilon_2 \\
 &- KMc\epsilon_1 + 2Mac\xi\epsilon_1 - Mc\xi^2\epsilon_2 + AMc\epsilon_1 - G_r K^2c \\
 &+ G_r Mc\xi + K^3e + K^2a\xi + KMe\xi - Ma\xi^2 + \\
 &Mc\xi\epsilon_1 + AK^2 - AM\xi + 2K^2e + K^2\xi - M\xi^2
 \end{aligned} \right) \\
 U(4) &= -\frac{\hspace{15em}}{24M(c\epsilon_2 + 1)(-\epsilon_1 c + K + 1)^2} \\
 T(0) &= c, T(1) = 0, T(2) = -\frac{\beta_r P_r g}{2c\epsilon_2 + 2}, T(3) = 0, T(4) = -1/8 \frac{\epsilon_2 \beta_r^2 P_r^2 g^2}{(c\epsilon_2 + 1)^3} \\
 W(0) &= d, W(1) = e, W(2) = \frac{K(b + 2d)}{2M}, W(3) = \frac{K}{6M} \left(2e + \frac{-c(a\epsilon_1 + G_r) - Ke + (a+1)\xi + A}{-\epsilon_1 c + K + 1} \right) \\
 W(4) &= \frac{K}{12M} \left(\frac{K(2d + b)}{M} - \frac{(c\epsilon_2 + 1)(Mb(\epsilon_1 c - \xi) + K^2(b + 2d)) + MP_r b\beta_r g\epsilon_1}{2M(c\epsilon_2 + 1)(-\epsilon_1 c + K + 1)} \right)
 \end{aligned}$$

The inverse transform of $Uk, T(k)$, and $W(k)$ are given as

$$u(y) = \sum_{k=0}^N U(k) y^k \tag{3.14}$$

$$\theta(y) = \sum_{k=0}^N T(k) y^k \tag{3.15}$$

$$\omega(y) = \sum_{k=0}^N W(k) y^k \tag{3.16}$$

which when substituted give;

$$\begin{aligned}
 & a + by + \frac{-c(a\epsilon_1 + G_r) - Ke + (a + 1)\xi + A}{-2\epsilon_1 c + 2K + 2} y^2 \\
 & - \frac{(c\epsilon_2 + 1)(Mb(\epsilon_1 c - \xi) + K^2(b + 2d)) + MP_r b\beta_r g\epsilon_1}{6M(c\epsilon_2 + 1)(-\epsilon_1 c + K + 1)} y^3 \\
 u(y) = & \left(\begin{aligned}
 & -2MP_r a\beta_r cg\epsilon_1^2 - Mac^3\epsilon_1^2\epsilon_2 - 2G_r MP_r \beta_r cg\epsilon_1 - G_r Mc^3\epsilon_1\epsilon_2 \\
 & -K^2ac^2\epsilon_1\epsilon_2 - 2K^2c^2e\epsilon_1\epsilon_2 - KMP_r a\beta_r g\epsilon_1 - 3KMP_r \beta_r eg\epsilon_1 \\
 & -KM c^2e\epsilon_1\epsilon_2 + 3MP_r a\beta_r g\xi\epsilon_1 + 2Mac^2\xi\epsilon_1\epsilon_2 + 3AMP_r \beta_r g\epsilon_1 \\
 & + AMc^2\epsilon_1\epsilon_2 - G_r K^2c^2\epsilon_2 - G_r KMP_r \beta_r g + G_r Mc^2\xi\epsilon_2 + K^3ce\epsilon_2 \\
 & + K^2ac\xi\epsilon_2 + KMce\xi\epsilon_2 - MP_r a\beta_r g\epsilon_1 + 3MP_r \beta_r g\xi\epsilon_1 - Mac^2\epsilon_1^2 \\
 & - Mac\xi^2\epsilon_2 + Mc^2\xi\epsilon_1\epsilon_2 + AK^2c\epsilon_2 - AMc\xi\epsilon_2 - G_r \beta_r P_r gM \\
 & - G_r Mc^2\epsilon_1 - K^2ac\epsilon_1 - 2K^2ce\epsilon_1 + 2K^2ce\epsilon_2 + K^2c\xi\epsilon_2 \\
 & - KMce\epsilon_1 + 2Mac\xi\epsilon_1 - Mc\xi^2\epsilon_2 + AMc\epsilon_1 - G_r K^2c \\
 & + G_r Mc\xi + K^3e + K^2a\xi + KMe\xi - Ma\xi^2 + \\
 & Mc\xi\epsilon_1 + AK^2 - AM\xi + 2K^2e + K^2\xi - M\xi^2
 \end{aligned} \right) y^4 \\
 & - \frac{\hspace{10em}}{24M(c\epsilon_2 + 1)(-\epsilon_1 c + K + 1)^2} y^4
 \end{aligned} \tag{3.17}$$

$$\theta(y) = c - \frac{\beta_r P_r g}{2c\epsilon_2 + 2} y^2 - \frac{\epsilon_2 \beta_r^2 P_r^2 g^2}{8(c\epsilon_2 + 1)^3} y^4 \tag{3.18}$$

and

$$\begin{aligned}
 & d + ey + \frac{K(b + 2d)}{2M} y^2 + \frac{K}{6M} \left(2e + \frac{-c(a\epsilon_1 + G_r) - Ke + (a + 1)\xi + A}{-\epsilon_1 c + K + 1} \right) y^3 \\
 \omega(y) = & \frac{K}{12M} \left(\frac{K(2d + b)}{M} - \frac{(c\epsilon_2 + 1)(Mb(\epsilon_1 c - \xi) + K^2(b + 2d)) + MP_r b\beta_r g\epsilon_1}{2M(c\epsilon_2 + 1)(-\epsilon_1 c + K + 1)} \right) y^4
 \end{aligned} \tag{3.19}$$

4 Results and Discussions

The solutions for the axial velocity, micro rotation component, pressure gradient, volumetric flow rate, and stream function with energy equation were obtained in the previous section for the cases when $r = 0, 1,$ and 2 . This section presents the results obtained graphically using some of the parameters as describe by [3, 6-8, 12, 14]. Figure 2 represents the variations of axial velocity with the height when $x = 0$ for different values of all other parameters of interest. It can be seen from Figure 2a that an increase in the magnetic parameter (H_a) reduces the flow of fluid at the two walls, but increases it towards the centre. It can be observe that at the walls of the channel, the flow started reducing and is more pronounced at the centre. This is as a result of the external magnetic force that was applied perpendicular to the flow. Figure 2b shows the effect of slip on the flow speed and it can be seen that the flow stratified incrementally near the channels as slip parameter is increasing and damping the flow of fluid at the middle. This evidence of slips parameter is well pronounce near the walls of the channel. Mention to be made of the reversal trend near the wall. This is due to the formation of the mucosa and submucosa layer in the stomach and the evidence of the airy-like tissues villi and micro-villi in the small intestine. Figure 2c describe the effect of porosity parameter (K_p) on the axial velocity. The effects of variable viscosity and variable thermal conductivity parameters are shown in Figures 2i and 2j. It is notice that increasing the variable viscosity parameter speeds-up the flow while increase in the variable thermal viscosity parameter slows-down the flow of the fluid. It can be noticed from Figure 2g that as the Grashof number (G_r) is increasing, the velocity is reducing while the reverse is notice for Prandtl number (P_r) in Figure

2h. The description of microrotation components were depicted in Figure 3. It will be noticed from Figures (3a, 3b, 3e, 3f, 3h) that the microrotation component increases as the governing parameters are increasing while Figures. (3c, 3d, 3g) reduces. Figures 5 and 4 show the effect of the governing parameters on the shear stresses τ_{xy} and τ_{yx} at both lower and upper walls of the channel. It will be notice that enhancing the magnetic (H_a), viscosity parameters (K) and thermal viscosity parameter ε_2 , increases the shear stresses at both walls of the channel. Reduction in shear stress at the two walls sets in with increasing porosity permeability (K_p), slip parameters (ζ), Prandtl (P_r), Graspof numbers (G_r) and viscosity parameter ε_2 which show that more deposition of enzymes at the passage of chyme reduce shear stress. Figure 6 describe the effects of the governing parameters on the pressure gradient $\frac{\partial p}{\partial x}$. It is clear from figures 6a and 6b that an increment in the slip ζ and viscosity parameters K increases the pressure gradient of the fluid and figures 6b, 6d, 6f and 6g show that the porous permeability, material constant, heat absorption parameters, Prandtl and Graphof numbers reduce the pressure gradient of the fluid. The graphs of pressure rise against positive slip parameter for different Hartmann number explain that the pressure rise decreases as the magnetic parameters is increasing as shown in Figure 7. It would be noticed from 7a, 7c and 7d that as the various parameters (Hartmann, Graphof and Prandtl numbers) were been varied for pressure rise against slip parameter, it impede the rise of the pressure while there is a pressure rise as the Graphof number is increasing. This reveals that a propulsion force will be required at the initial point before the involuntary movement (from the oesophagus through to the rectum) and when ejecting the waste product (undigested food through the anus).

The stream functions for various parameters of relevance are depicted in Figures [8-13]. By a given wave length, the distribution of stream lines pattern in the presence of magnetic field is shown in Figure 8. It was discovered that when the size of the wall shrinks, the production of bolus magnetic parameters H_a rises. It's worth noting in Figure 9 that as the slip parameter ζ is increased, the trapped bolus shrinks in size and eventually evaporates. As a result, the magnetic field strength and slide effects work together to prevent trapped bolus formation. The distribution of streamlines at various diverging angles is shown in Figure 10. We notice that as θ increases, the trapped bolus on both sides of the channel's central line grows in size. However, as seen in Figure 11, the porous medium permeability parameter K_p continues to create more closed streamlines at the wall. As shown in Figure 12, more bolus are generated near the channel of the walls. The distribution of stream functions against the Prandtl number is shown in Figure 13. This demonstrates that when the Prandtl number rises, more bolus form along the fluid's flow channel.

5 Conclusion

The effects of slip velocity and heat transfer on the peristaltic transport of physiological fluids represented by a micropolar fluid model traveling through a non-uniform porous channel are investigated in this work. The study of velocity distribution, pumping features, variable and thermal viscosity and trapping phenomena has received considerable attention in this investigation. The present research leads to the critical conclusion that by adding an external magnetic field is feasible to enhance pumping action (pressure gradient) as often as necessary, and that bolus development can be reduced to a significant level. At the bottom and higher sides of the channel walls, shear stresses τ_{xy} and τ_{yx} increase as the magnetic parameter H_a increases. The production of trapped bolus is slowed down by the slip velocities (ζ , ε_1 , and ε_2) near the wall. As a result, the findings shed some light on issues such as gastrointestinal fluid movement, intra-uterine fluid motion generated by uterine contraction, and flow through small blood arteries and intrapleural membranes.

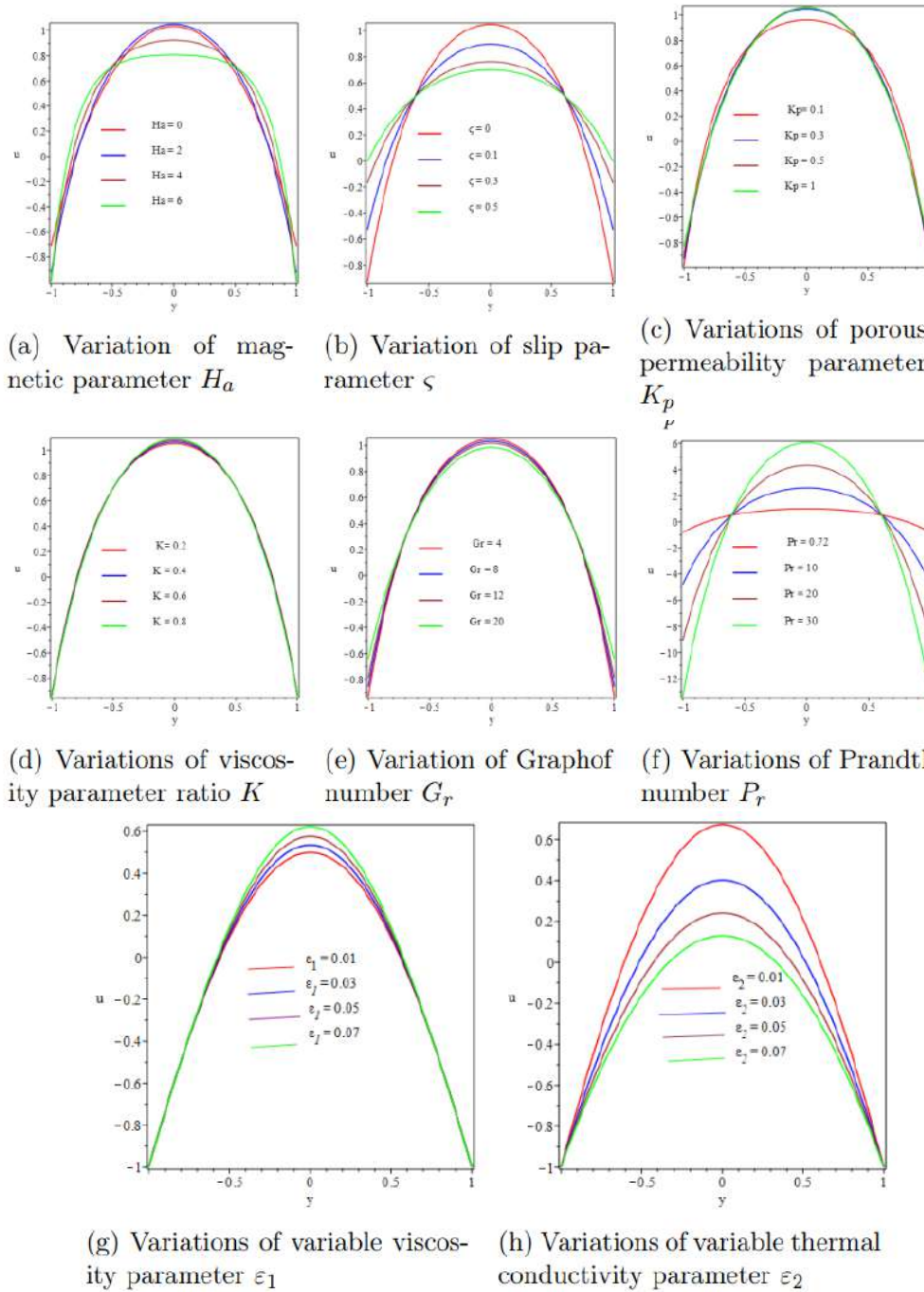


Figure 2: Graphs of axial velocity with varying parameters of interest

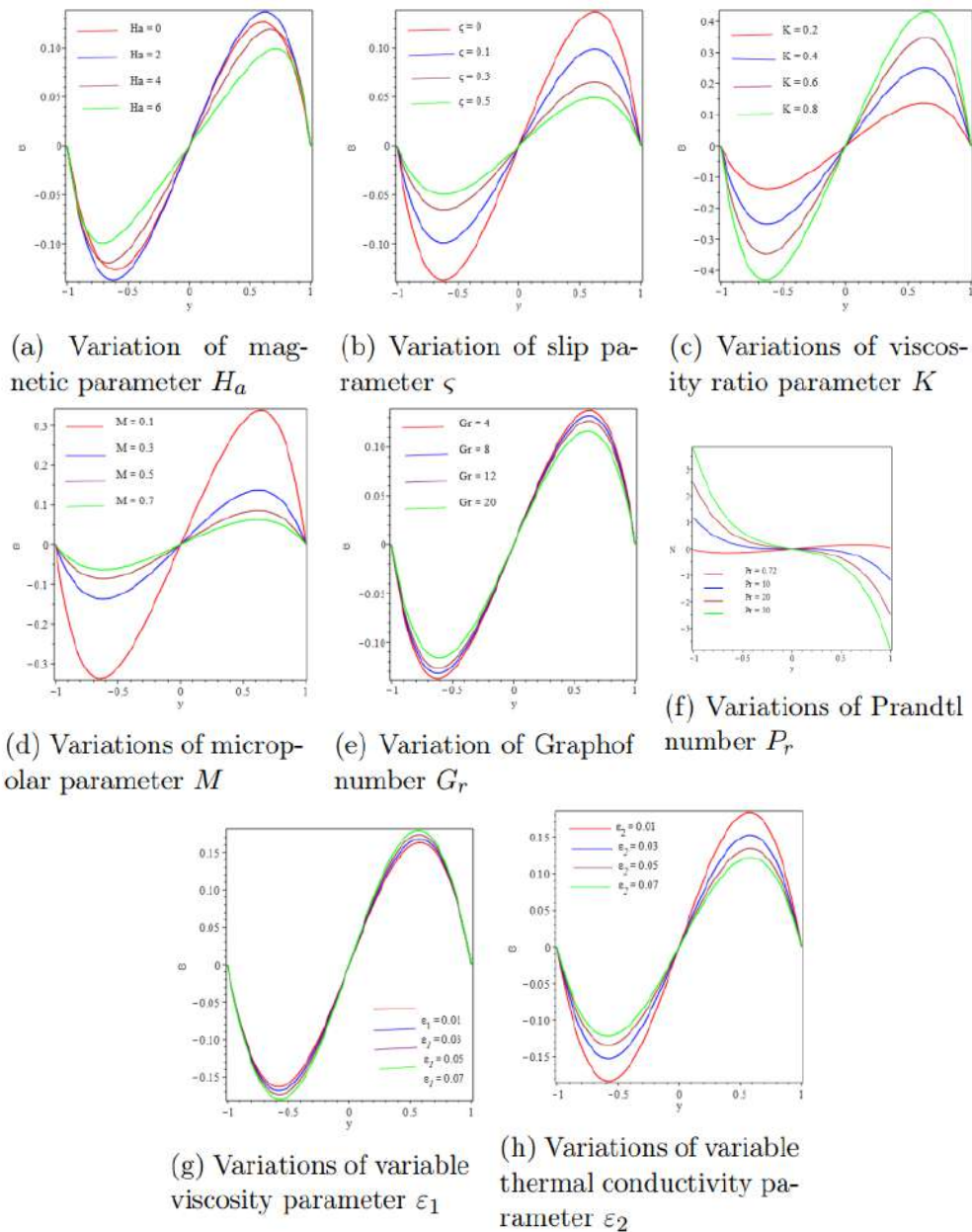


Figure 3: Graphs of microrotation component with varying parameters of interest

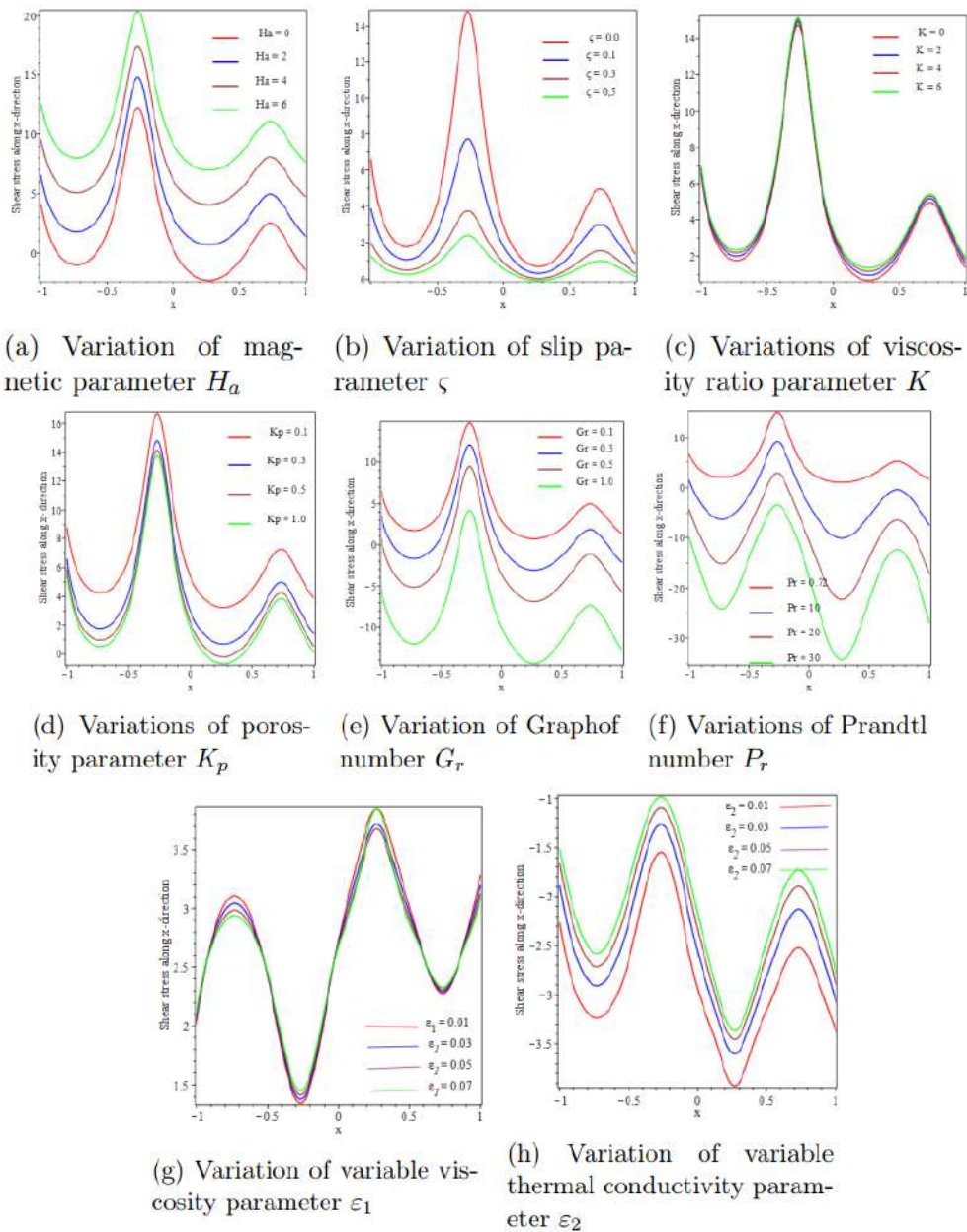


Figure 4: Graphs of wall shear stress τ_{xy} at the lower wall of the channel

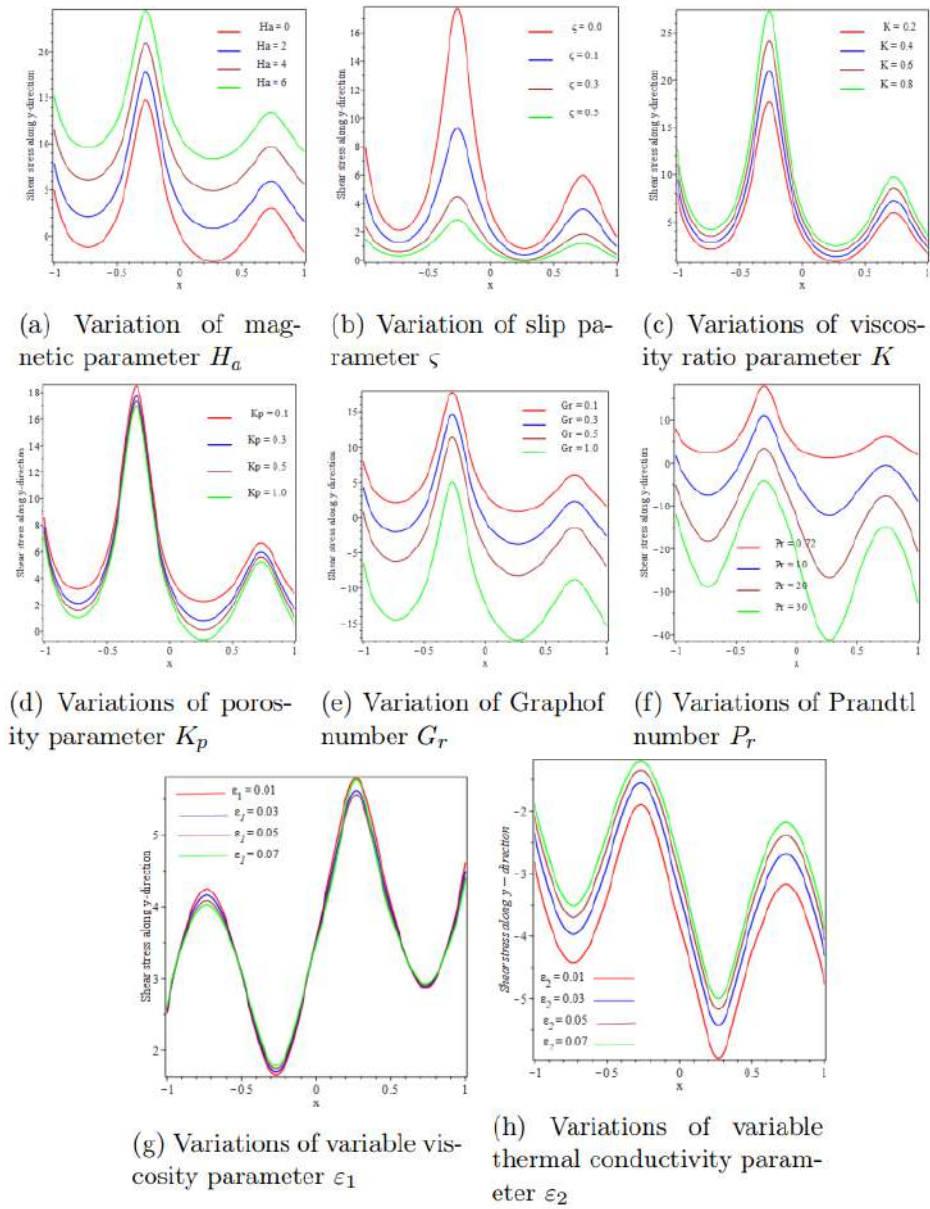


Figure 5: Graphs of wall shear stress τ_{yx} at the lower wall of the channel

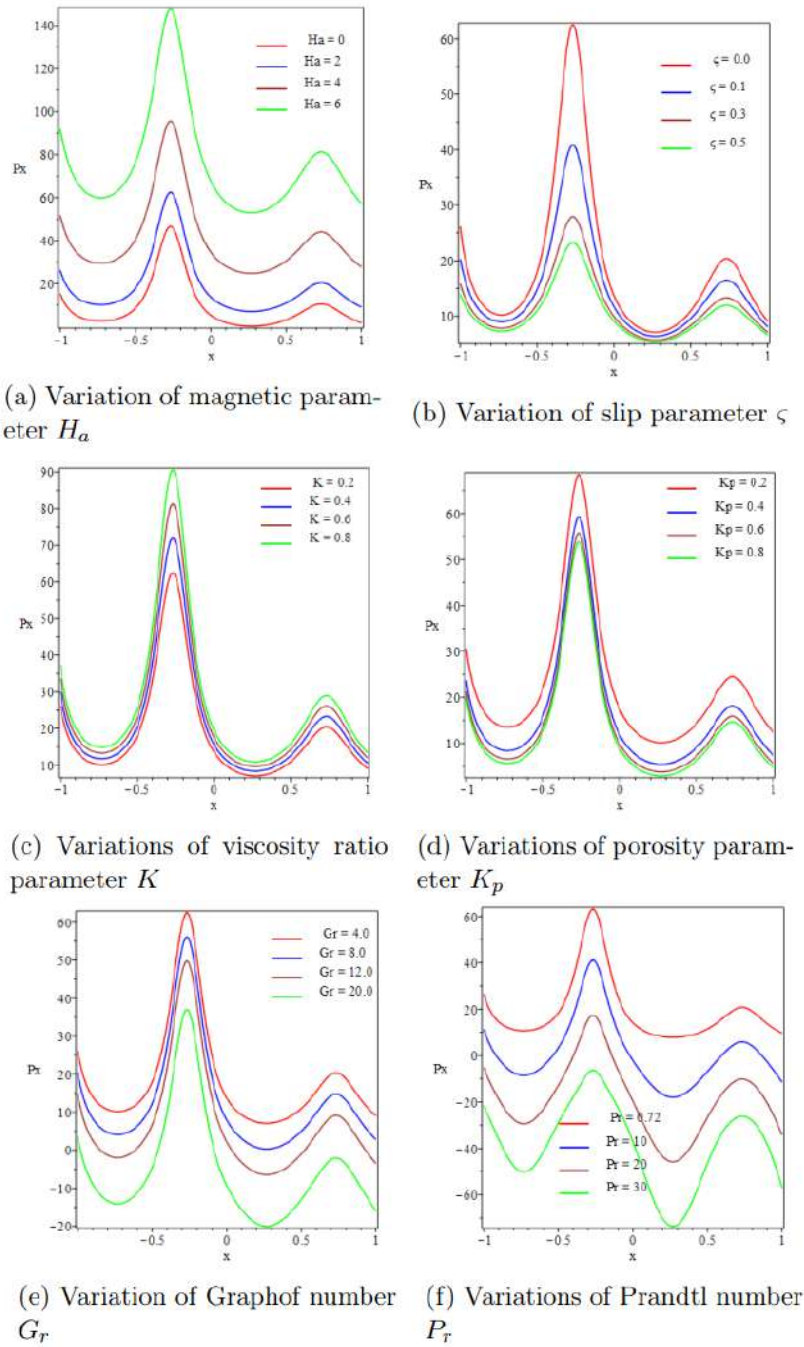


Figure 6: Distribution of pressure gradient

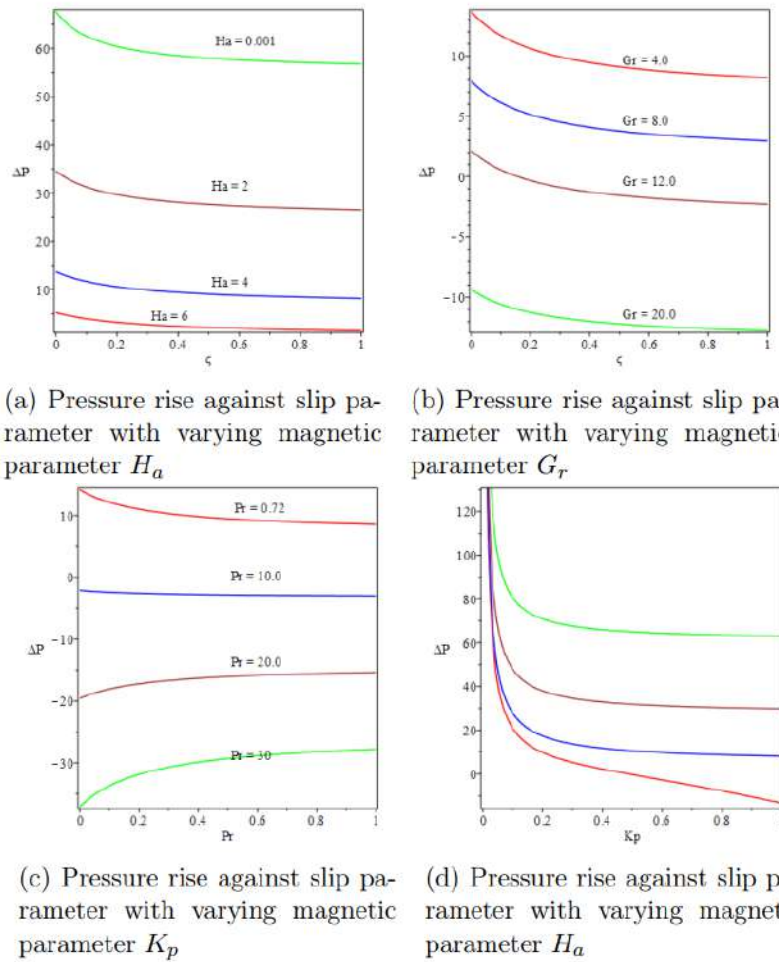
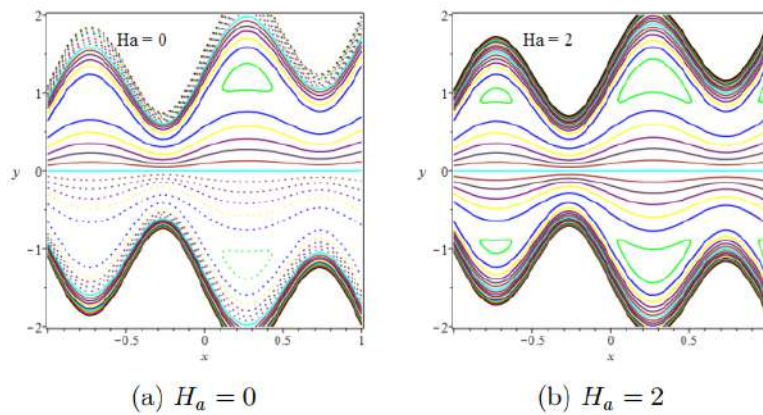


Figure 7: Graph of pressure rise



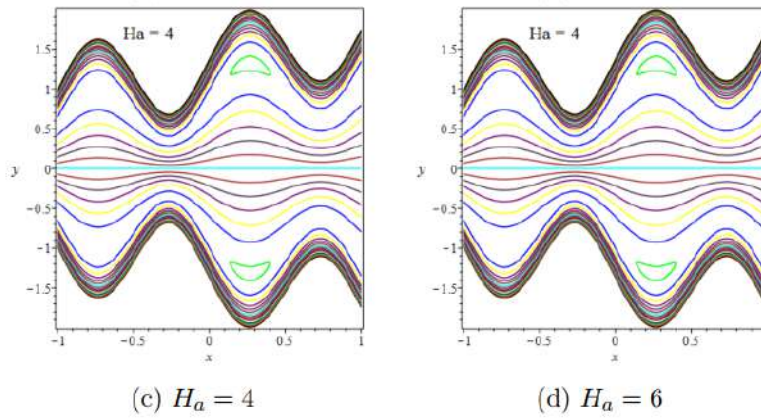


Figure 8: Distribution of streamlines for different Hartman number H_a

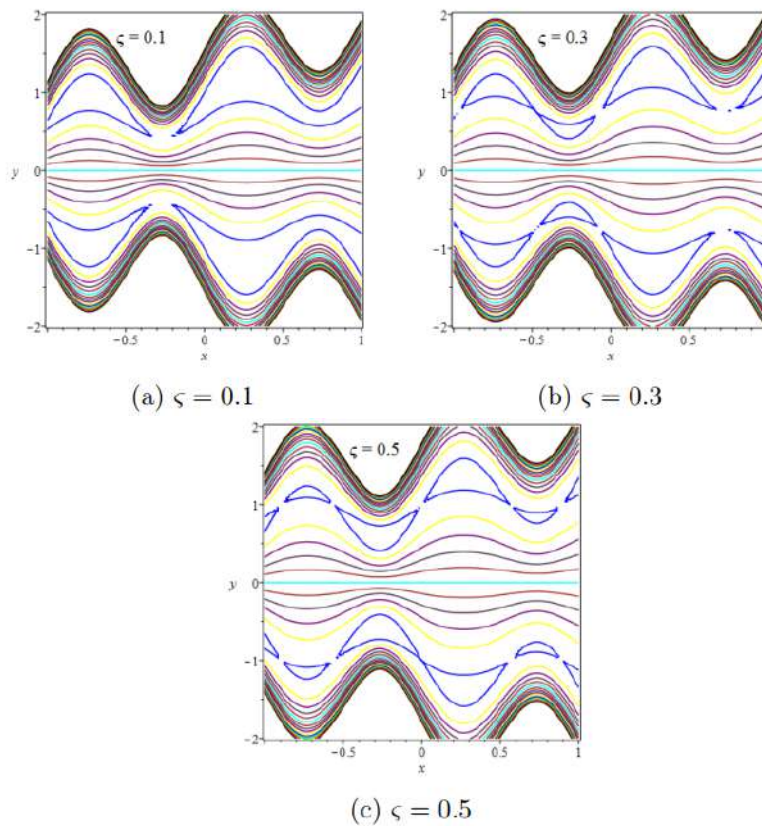


Figure 9: Distribution of streamlines for different slip parameters ζ

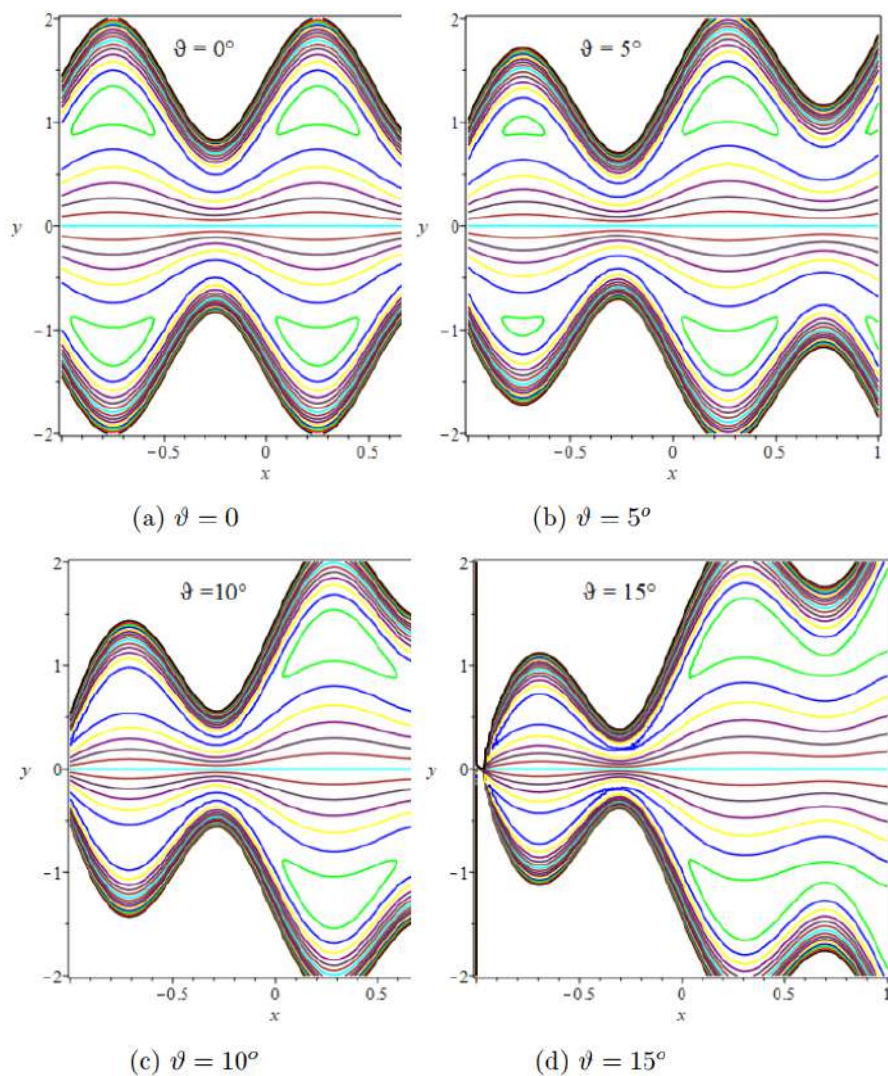
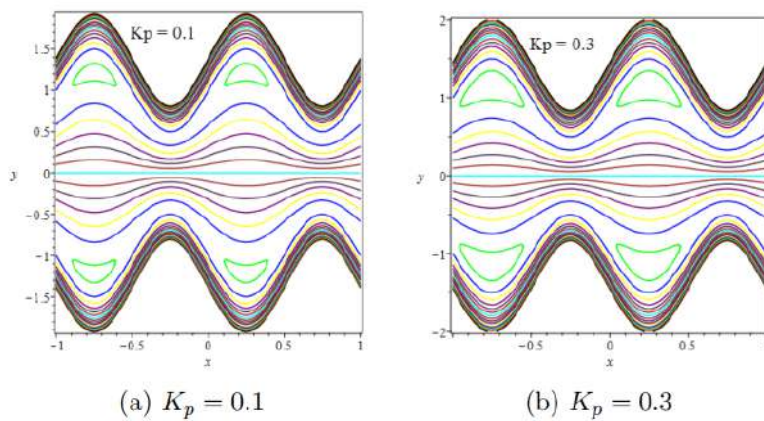


Figure 10: Distribution of streamlines for different tilt angle ϑ



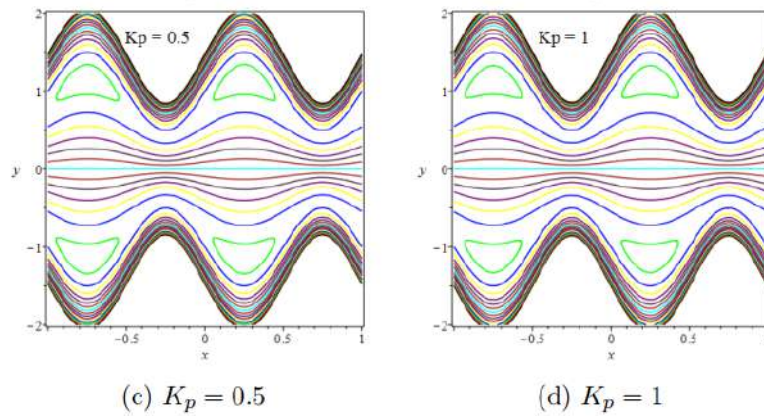


Figure 11: Distribution of streamlines for different permeability K_p

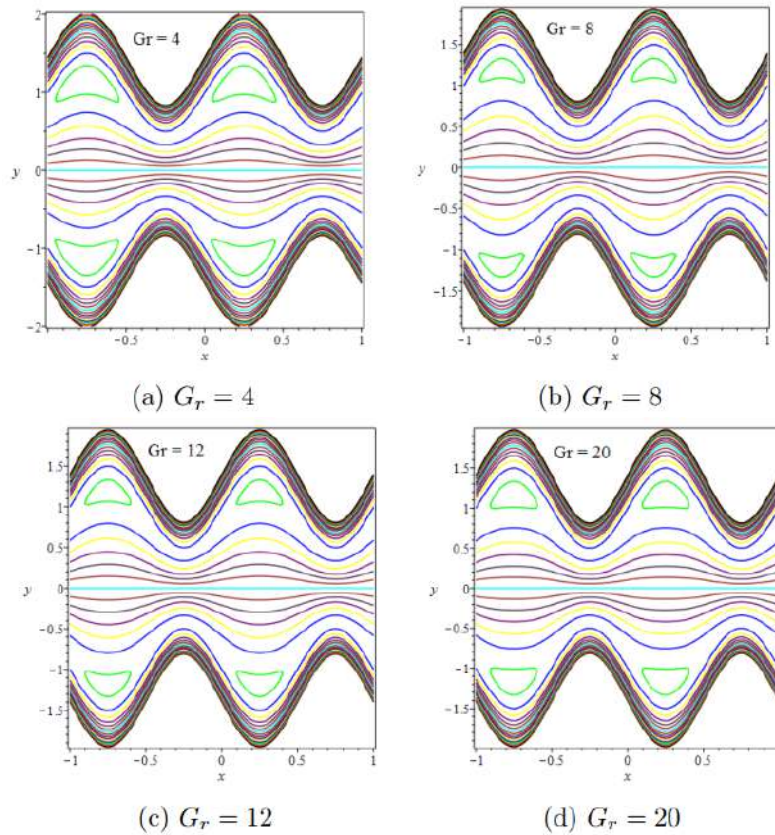


Figure 12: Distribution of streamlines for different Graphof number G_r .

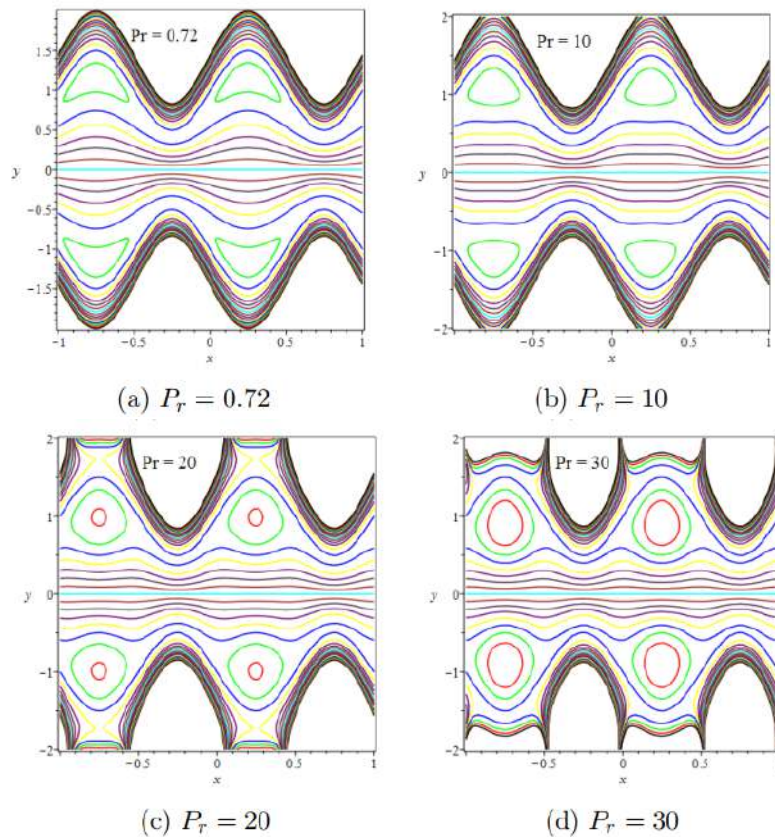


Figure 13: Distribution of streamlines for different Prandtl number P_r

Conflicts of Interest

No conflict of interest was declared by the authors.

References

- [1] Vishnyakov, V. I. & Pavlov, K. B. Peristaltic flow of a conductive liquid in a transverse magnetic field. *Magnetohydrodynamics* **8**, 174–178 (1972).
- [2] Eringen, A. C. Theory of micropolar fluids. *Journal of Mathematics and Mechanics* 1–18 (1966).
- [3] Ali, Nasir & Hayat, Tasawar Peristaltic flow of a micropolar fluid in an asymmetric channel. *Computers & Mathematics with Applications*. **55**, 589–608 (2008).
- [4] Ariman, TTND, Turk, MA & Sylvester, ND. Applications of microcontinuum fluid mechanics. *International Journal of Engineering Science*. **12**, 273–293 (1974).
- [5] Chaube, MK, Pandey, SK & Tripathi, D. Slip effect on peristaltic transport of micropolar fluid. *Appl. Math. Sci.* **4**, 2015–2117 (2010).
- [6] Shit, G. & Roy, M. Effect of slip velocity on peristaltic transport of a magneto-micropolar fluid through a porous non-uniform channel. *International Journal of Applied and Computational Mathematics* **1**, 121–141 (2015).

- [7] Shit, G. C., Roy, M. & Ng, E. Y. K. Effect of induced magnetic field on peristaltic flow of a micropolar fluid in an asymmetric channel. *Acta Mechanica* **26**, 1380–1403 (2010).
- [8] Shit, G. C. & Roy, M. Hydromagnetic effect on inclined peristaltic flow of a couple stress fluid. *Alexandria Engineering Journal* **53**, 949–958 (2014).
- [9] Chandra, S. & Pandey, S. K. A study on peristaltic flow of micropolar fluids: An application to sliding hiatus hernia. *Journal of Physics: Conference Series* **1141**, 012092 (2018).
- [10] Rana, B. M. J., Arifuzzaman, S. M., Reza-E-Rabbi, S. K., Ahmed, S. F. & Khan, M. S. Energy and magnetic flow analysis of Williamson micropolar nanofluid through stretching sheet. *International Journal of Heat and Technology* **37**, 487–496 (2019).
- [11] Muthu, P., Kumar, B. & Chandra, P. Peristaltic motion of micropolar fluid in circular cylindrical tubes: Effect of wall properties. *Applied Mathematical Modelling* **32**, 2019–2033 (2008).
- [12] Shit, G. C., Ranjit, N. K. & Sinha, A. Adomian decomposition method for magnetohydrodynamic flow of blood induced by peristaltic waves. *Journal of Mechanics in Medicine and Biology* **17**, 1750007 (2017).
- [13] Misra, J. C. & Pandey, S. K. Peristaltic transport of blood in small vessels: study of a mathematical mode. *Computers & Mathematics with Applications* **43**, 1183–1193 (2002).
- [14] Pandey, S. K. & Chaube, M. K. Peristaltic flow of a micropolar fluid through a porous medium in the presence of an external magnetic field. *Communications in Nonlinear Science and Numerical Simulation* **16**, 3591–3601 (2011).
- [15] Afsar Khan, A. and Ellahi, R. & Vafai, K. Peristaltic transport of a Jeffrey fluid with variable viscosity through a porous medium in an asymmetric channel. *Advances in Mathematical Physics* **2012**, (2012).
- [16] Rao, A. R. & Mishra, M. Nonlinear and curvature effects on peristaltic flow of a viscous fluid in an asymmetric channel. *Acta Mechanica* **168**, 35–59 (2004).
- [17] Massoudi, M. & Christie, I. Effects of variable viscosity and viscous dissipation on the flow of a third grade fluid in a pipe. *International Journal of Non-Linear Mechanics* **30**, 687–699 (1995).
- [18] Pakdemirli, M. & Yilbas, B. S. Entropy generation for pipe flow of a third grade fluid with Vogel model viscosity. *International Journal of Non-Linear Mechanics* **41**, 432–437 (2006).
- [19] Balachandra, H., Rajashekhar, C., Mebarek-Oudina, F., Manjunatha, G., Vaidya, H. & Prasad, K. V. Slip Effects on a Ree-Eyring Liquid Peristaltic Flow Towards an Inclined Channel and Variable Liquid Properties. *Journal of Nanofluids*. **10**, 246–258 (2021).
- [20] Fatunmbi, Ephesus Olusoji, Mabood, Fazle & Adeniyani, Adetunji Stagnation-Point Flow of Magneto-Williamson Nanofluid over a Stretching Material with Ohmic Heating and Entropy Analysis. *International Journal of Mathematical Sciences and Optimization: Theory and Applications* **7**, 131–145 (2021).
- [21] Zhou, J. K. Differential Transformation and Its Applications for Electrical Circuits. *Huazhong University Press, Wuhan, China* (1986).
- [22] Sobamowo, M. G., Yinusa, A. A., Adeleye, O. A., Alozie, S. I., Salawu, S. A. & Salami, M. O. On the Efficiency of Differential Transformation Method to the Solutions of Large Amplitude Nonlinear Oscillation Systems. *World Scientific News* **139**, 1–60 (2020).
- [23] Sobamowo, G. M., Jayesimi, O. & Waheed, A. On the study of magnetohydrodynamic squeezing flow of nanofluid between two parallel plates embedded in a porous medium. *Computational Engineering and Physical Modeling* **1**, 1–15 (2018).